Comparative Study of Positioning HBM to Cycling Postures Based on Experimental Data

Maria Oikonomou[1], Athanasios Lioras[2], Lambros Rorris[3], Thomas Nikodelis[1], Athanasios Mihailidis[1]

[1]Aristotle University of Thessaloniki
[2]BETA CAE Systems SA
[3]BETA CAE Systems International AG

1 Abstract

The objective of Crash Analysis is to ensure the safety of a diverse spectrum of road users through the utilization of several finite element (FE) crash simulations. While a considerable number of studies have focused on evaluating the motion and the potential injuries of occupants and pedestrians, the investigation of two-wheel vehicle users remains underrepresented, even though they are considered vulnerable road users and two-wheelers are common personal transportation. Therefore, studying their kinematic behavior in multiple collisions is crucial to ensure safe and convenient travel.
A limited number of studies dedicated to two-wheelers are conducted using Human Body Models (HBMs), even though they are deemed the most proper way to explore human behavior in various crash scenarios. HBMs are generated in the seating and standing postures, representing the occupant and pedestrian accordingly, and consequently, the articulation of the HBMs to adopt the distinct cyclist posture is challenging. Thus, the comprehensive evaluation of cyclists' safety using HBMs entails the resolution of several difficulties.
This study undertakes the exploration of distinct ways of identifying cyclists' postures by employing different data collection processes. A comparison between the data collection methods is executed to specify the most rational approach. Furthermore, this study develops an articulation method that positions the HBM in a target posture. Thus, the HBM is positioned in the cyclist's target posture using data computed by the chosen data collection method. The acquired knowledge will facilitate the investigation of unique non-standard initial positions and contribute to the extensive examination of cyclists' behavior in multiple crash situations using HBMs.
The study was conducted in LS-DYNA, using the THUMS M50 HBM. The positioning process IS developed in ANSA Python scripts and using the ANSA HBM Articulation tool.

***KEYWORDS: Human Body Models (HBMs), Positioning, Vulnerable Road Users (VRU), Two-wheelers, Bicyclist**

2 Introduction

The expanding use of two-wheel vehicles and the escalating frequency of traffic accidents involving them have underlined the necessity of the in-depth study of the kinematic behavior of cyclists across multiple collision scenarios. The two-wheelers category generally embraces a wide range of vehicles, including motorcycles, bicycles, scooters, e-bikes, and others. However, given the rapid increase in their usage, this study focuses on bicycles. Still, an identical methodology is applicable to any form of two-wheeler.
The investigation into bicyclists' safety is beneficial both at the individual and societal levels. Such an investigation contributes to the holistic comprehension of the accidents' influential factors, potentially leading to the identification of strategic measures aimed at mitigating such incidents. The strategies in question span a spectrum of interventions, ranging from the optimization of bicyclist safety equipment, such as bicyclist helmets and protective scarves [1], [2], to the redesign of diverse vehicle attributes and extending to the augmentation of cycling infrastructure and urban planning. Moreover, the establishment of a secure cycling environment will encourage more people to cycle, thereby promoting sustainable transportation, being environmentally conscious, and contributing to the development of a healthier lifestyle characterized by physical activity.

2.1 Bicyclists in Literature

Within the literature, numerous investigations center around bicyclists. However, only a limited subset of them analyzes their kinematic characteristics and behavior responses in collision scenarios. In contrast, most of them direct their attention towards disparate aspects. For instance, the study [3] examines bicyclists' perceived level of safety and their willingness to bicycle in different cycling

© 2023 Copyright by DYNAmore GmbH, an Ansys Company

environments using bicycle simulators. In parallel, the study [4] focuses on the classification of different road users through a traffic monitoring technique, enabling the exploration of bicyclist interaction with motorized vehicles and potentially revealing insights into crash mechanisms. The investigation of bicyclists' kinematics and injury entails the examination of experimental field data, as referenced in [5], [6], or the execution of crash simulations, as analyzed below.

2.2 Human in Crash Analysis

In the context of crash simulation methodologies, bicyclists are commonly represented via human multibody models, crash test dummies, or FE human body models, each characterized by distinct strengths and limitations. Human multibody models offer valuable insights into the forces and accelerations experienced in different body parts. Yet, their application is constrained by their simplified depiction of the human body, as they fail to capture individual anatomical structures. Consequently, this limitation impacts the accuracy of the analysis. Typically, as in references [7], [8], [9], [10], multibody models are deployed to investigate kinematic attributes and targeted head injury metrics.
Conversely, crash test dummies are capable of physical validation performed through real-world crash tests. Thus, dummies can be used to validate the outcomes of FE simulations (utilizing dummies or HBMs) or multibody simulations using human multibody models. However, the applicability of crash test dummies is constricted by their limited biofidelity, as they fail to represent each anatomical human part separately, and they are unable to capture the entire human kinematics. Moreover, crash test dummies are designed for specific crash scenarios and cannot be representative of a broad spectrum of crash occurrences. Some noteworthy instances of research involving crash test dummies to investigate cyclists' kinematic response and injury behavior are [11], [12], [13], [14].
Lastly, HBMs exhibit a heightened level of anatomical fidelity, enabling the accurate emulation of diverse kinematic responses and the in-depth exploration of injury phenomena. HBMs incorporate complex material models, thereby approximating the properties of authentic human tissues. Furthermore, they possess the adaptability to be modified to represent various individuals, enabling an individualized analysis approach. However, HBMs have limitations in terms of high computational demands and the need for extensive validation procedures. Generally, HBMs are acknowledged as state-of-the-art human representation models, as they find utility in a wide spectrum of crash scenarios and can provide detailed outcomes for both kinematics and injury. Thus, this study will focus on investigating crash analysis conducted through HBMs. Selected studies dedicated to the analysis of cyclist-related crashes that harness the capability of HBMs are [1], [2], [14], [15], [16].

2.3 Studied Parameters in Crash Analysis

Crash simulations provide a means to explore various parameters amenable to manipulation within crash scenarios. Literature frequently engages in the examination of several parameters related to crash characteristics. To exemplify references [2], [7], [10], [15] study the affection of collision speed in cyclists' kinematics and resultant injuries, while [2], [7], [10], [15], [17] delve into the influence of collision angle. Additionally, a significant number of publications undertake the examination of a variety of vehicle parameters, including vehicle type [7], [9], [10], [13], [15], [16], vehicle speed [6], [9], [13], [15], [17], and vehicle mass [6]. Concurrently, careful examination is focused on various factors relative to bicycles. For instance, attributes like bicycle type [14], bicycle speed [6], [15], bicycle mass [6], rider's protection [2], [6], rider's posture [9], and pedal position [2], [13] are issues to comprehensive examination. Moreover, multiple comparative analyses regarding the kinematic behavior and injury patterns of cyclists with varying attributes [1], [9], [13], [16], such as size and gender, or comparisons between cyclists of different two-wheelers [9], [14], [16], and even contrast between cyclists and pedestrians' behavioral patterns [7], [10], [13] are frequently undertaken across numerous investigations.

However, to capture a realistic kinematic behavior of the cyclist that will result in an accurate injury prediction, one of the most essential steps is to accomplish the cyclist's initial position. Thus, this study investigates and compares two different skin marker methods to collect sufficient data about the bicyclist's posture in the real world. The next critical step to continue with the crash simulation process is the articulation of the selected HBM in the previously specified posture, a highly challenging process. Therefore, this study develops an articulation method aimed at positioning the HBM in a cyclist's target posture.

3 Methods

The reproduction of body posture is the accurate positioning of HBM to replicate the experimentally derived Subject's position. The correlation between the HBM and the Subject is established by

© 2023 Copyright by DYNAmore GmbH, an Ansys Company

identifying reference points on the bones, commonly referred to as anatomical landmarks. The replication of body posture is based on the accurate positioning of the anatomical landmarks. Therefore, an essential step in producing an identical pose between the HBM and the reference Subject entails the definition of corresponding anatomical points on both Subject and HBM's Bones. Additional details regarding these anatomical landmarks are provided subsequently.
The extraction of the coordinates for the Subject's landmarks is typically facilitated through the utilization of skin markers or imaging techniques. While Imaging techniques possess the capability to determine the position of bones directly as required, skin markers do not possess this direct capability. Thus, the implementation of a skin marker method necessitates supplementary measurements of the Volunteer's skinfold thickness. This supplementary data is central in adapting the coordinates of skin markers as if they were set on the Volunteer's bones.
Within the scope of this study, an experimental investigation is conducted involving the simultaneous application of two distinct skin marker methodologies. The objective is to compute the 3D marker coordinates using both methods, compare their outcomes, and determine the more convenient approach. These methodologies denoted as the 'Conventional Stereo Vision Method' and the 'Optoelectronic Method,' will be comprehensively presented below.
The investigation involves a city bicycle with known typical dimensions and a volunteer exhibiting analogous physical attributes (height and weight) to those of the HBM intended to position. The chosen for positioning HBM is the THUMS AM50.
Then, upon computation of the 3D markers' coordinates, a caliper measures skinfold thickness on the prior markers' positions. Then, the HBM is articulated to attain the desired position as defined by the selected methodology and modified by skinfold measurements. The articulation procedure is conducted in LS-DYNA and uses ANSA Python scripts and the Ansa HBM Articulation tool. Further information regarding the positioning methodology will be provided in subsequent sections.

3.1 Anatomical Landmarks

Anatomical landmarks are the referenced points used to relate the HBM and the Subject. These points are easily recognizable and palpable on human bones, providing the sites where skin markers are affixed. Their selection is based on literature [18], [19], [20]. Some of the selected anatomical points are depicted in Figure 1. Multiple anatomical landmarks are selected in the upper extremities, lower extremities, head, pelvis, and spinal curvature.

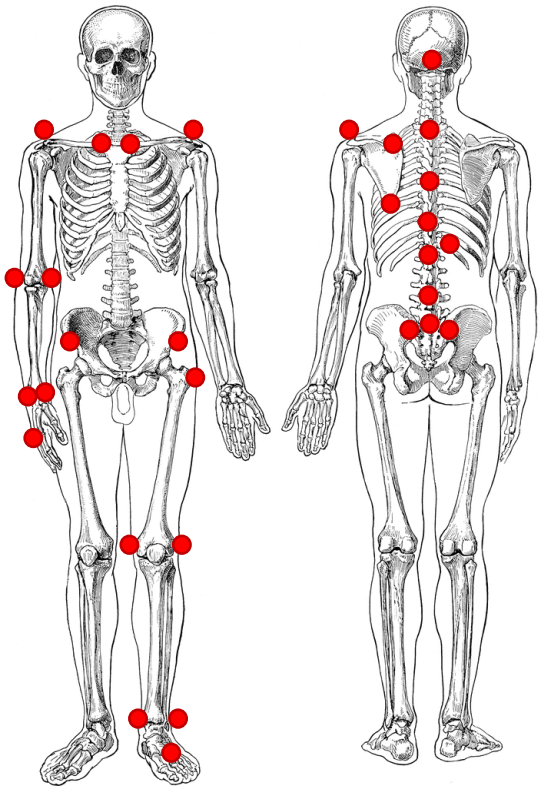

Fig.1: Anatomical Landmarks marked on human skeleton. (The skeleton image was taken from The Human Skeleton | ClipArt ETC (usf.edu).)

© 2023 Copyright by DYNAmore GmbH, an Ansys Company

3.2 Data Collection Methodologies

3.2.1 Conventional Stereo Vision Method

Generally, the Stereo vision method implements at least two cameras and, by knowing the relative position and orientation, enables the calculation of the 3D world coordinates of points visible in both cameras.
The conventional stereo vision system consisted of two conventional video cameras, each with a resolution of 1920x1080 pixels. The cameras are strategically placed with an approximate angle of 45 between their optical axes and centered on the bicycle saddle to ensure the depiction of the whole model, encompassing both the bicycle and the bicyclists.
The camera's intrinsic parameters were derived through a calibration process. The calibration process spans the entire model's volume, containing bicycle and bicyclist, and is executed by moving a calibration plane with sides measuring 1 meter in length at three parallel locations. The calibration is conducted using 21 points with known 3D coordinates. The digitization of the two camera views is performed three times by a proficient analyst utilizing custom-built analysis software. The average digitized points' image coordinates 'U' and 'V' are considered across the three repetitions. The outcome of these steps results in a calculated error within the range of 0.1 to 0.4 cm for the known reference points, while the computed coordinates of the unknown points exhibit errors ranging between 0.2 and 0.6 cm.

3.2.2 Optoelectronic Method

The second approach involves the utilization of an Optoelectronic system facilitated by the Optitrack v2.3 software. The system is equipped with 8 Flex-3 cameras with a pixel resolution of 640x480, and the 3D coordinates of anatomical landmarks are derived by combining the captures of all cameras. This method requires the implementation of reflective markers on Volunteer's anatomical landmarks.
Before taking the measurements, a calibration procedure is imperative. A stick equipped with three reflective markers placed in known distances is employed for the calibration. The stick is moved to cover the entire spatial volume of the model. The calibration accuracy is established by consistently computing the distances between these three markers. The resultant accuracy is lower than 0.2 mm for a length of 500mm.

3.2.3 Comparison of Data Collection Methods

A comparative assessment between the Conventional Stereo Vision Method and the Optoelectronic Method methods is conducted by evaluating markers computed through both methodologies. Specifically, the inter-marker distances are determined based on the 3D coordinates of each technique. Then, the percentage difference of these distances is derived.

3.3 HBM Positioning

Due to anatomical differences between the HBM and the Subject, the HBM's articulation cannot occur by directly using the coordinates of the previously defined Subject's anatomical points. As a result, the objective entails the articulation of the HBM in a manner that achieves the same slopes between its successive points with the Subject's successive markers. To accomplish this, an optimized iterative articulation method is devised to calculate the slopes' differences during each articulation iteration at each joint.
Depicted in Figure 2 are the kinematic joints participating in the articulation process. Within this visual representation, the colored bones denote the initial position of the HBM, whereas the gray figures illustrate an articulated posture. Regarding the upper limb region, articulation is realized across the radiocarpal joint, the humerus, the glenohumeral joint, and the radioulnar joint. The talocrural joint, the knee, and the acetabulofemoral joint can be articulated in the lower limb region. Moreover, the articulation extends to the individual movement of each lumbar vertebra, thoracic region, cervical region, and pelvis.
The articulation Procedure uses ANSA Python scripts and the ANSA HBM Articulation tool. The final HBM position is chosen as the one with the minimum slope error. An equivalent bike to the one used in the experiment is constructed using the ANSA Bicycle Configurator Tool.

© 2023 Copyright by DYNAmore GmbH, an Ansys Company

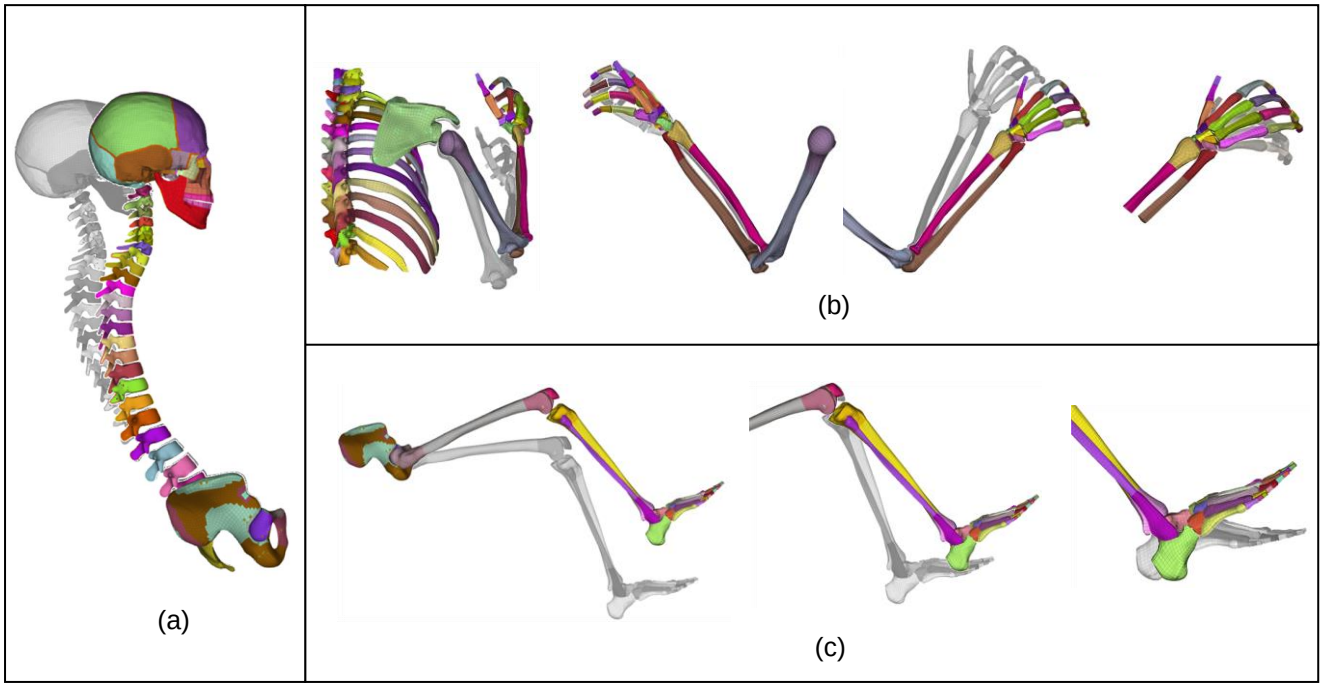

Fig.2: Kinematic joints participating in the articulation of the HBM in: (a) spine region, (b) upper extremities, (c) lower extremities. The colored bones show the initial position of the THUMS M50 HBM, while the gray figures illustrate an articulated posture of it.

4 Results

4.1 Comparison of Data Collection Methods

A comparative evaluation between the Conventional Stereo Vision Method and the Optoelectronic Method was undertaken. The analysis revealed that the maximum percentage difference in inter-marker distances is approximately 5%. This significantly low percentage suggests that both methods can accurately measure marker coordinates.
The Conventional Stereo Vision Method necessitates less intricate equipment, in contrast with the Optoelectronic method, which requires specialized software. However, the first method can precisely compute the markers' coordinates visible in both cameras, thus imposing limitations on marker placement locations on the Subject's body. Conversely, the Optoelectronic Method, employing 8 cameras, remarkably minimizes occluded areas, enabling markers to be placed across various body regions of the Subject. Furthermore, the manual digitization of images in the Conventional Stereo Vision Method could introduce slight inaccuracies in marker coordinates. Moreover, this method requires substantially more time for both the calibration phase and the extraction of 3D coordinates. Considering these factors, the Optoelectronic Method emerges as the most convenient to use. Consequently, the entire set of bicyclist measurements was conducted using this method.

4.2 Positioning Results

The automated positioning procedure was implemented utilizing experimental data. This dataset comprises the 3D coordinates of markers obtained through the Optoelectronic Method, along with measurements of skinfold thickness taken at the corresponding marker locations. In Figure 3, on the left, the Subject riding the city bike is illustrated. On the right-hand side, the ultimate final HBM's posture is presented. First, the HBM bones and then the whole HBM body are shown. The last illustration combines the HBM skeletal structure with the Subject's position curves. These curves are formed by interconnecting successive markers, adjusted according to skinfold thickness measurements, allowing for direct comparative analysis of the HBM and the Subject. As we can observe, the HBM closely approximates the reference Subject's curves. The maximum absolute slope difference between the Subjects' and HBM's successive markers is around 5 degrees for arms, legs, and spine regions.

© 2023 Copyright by DYNAmore GmbH, an Ansys Company

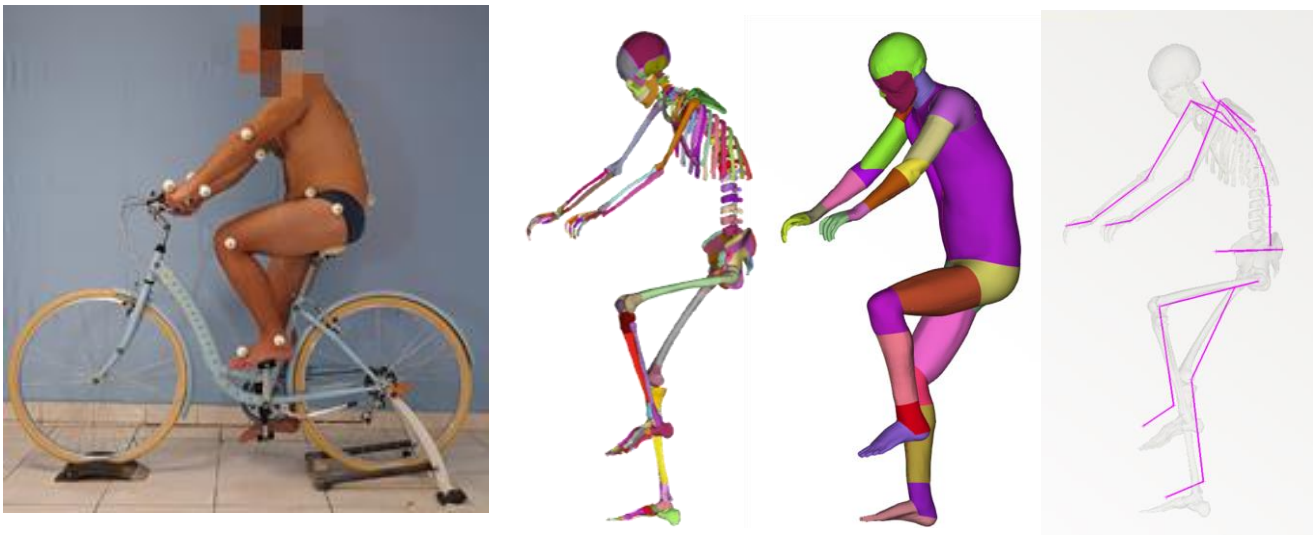

(a) (b) (c) (d)

Fig.3: THUMS M50 HBM articulation in Subject's bicyclist posture. (a) Subject riding the city bike is illustrated. (b) HBM's Bones articulated in Subject's bicyclist posture. (c) HBM's Body articulated in Subject's bicyclist posture. (d) Combination of HBM's Bones in Subject's bicyclist posture and Subject's position curves.

5 Summary

This study undertakes the exploration of distinct ways of identifying cyclists' postures by employing different data collection processes. A comparative analysis between these distinct data collection methods is conducted to ascertain the most convenient one. The outcomes of this comparative assessment indicate that the Optoelectronic Method exhibits a significant level of convenience, while both Optoelectronic and Conventional Stereo Vision Methods display satisfactory accuracy levels.
In addition, this study presents a novel technique for positioning the HBM in a target cyclist's posture as defined by experimental data. The data can be derived from any volunteer matching the features of the to-be-positioned HBM. The acquired knowledge facilitates the exploration of unique non-standard initial positions, contributing significantly to the extensive investigation of cyclists' behavior across various crash situations employing HBMs.
It's important to note that the automated positioning process can be universally applied, extending beyond cyclist-specific postures. Thus, this method enables the examination of diverse initial positions, ensuring human safety in non-standard load cases.

6 Literature

[1] Alvarez, V., Wendelrup, H., Brolin, K.: "Analyzing bicycle accidents with human body models ", 13th European LS-DYNA Conference, 2021, 134-135.
[2] Alvarez, V., Malalla, A., Säther, A., Olsson, D., Jonsson, T., Brolin, K.: "Predicting Head and Neck Injury in Bicycle Accident Simulations", HUMAN MODELING AND SIMULATION IN AUTOMOTIVE ENGINEERING Conference, 2022.
[3] Nazemi, M., Van Eggermond, M. A. B., Erath, A., Schaffner, D., Joos, M., Axhausen, K. W.: "Studying bicyclists' perceived level of safety using a bicycle simulator combined with immersive virtual reality", Accident Analysis & Prevention, 2021, 151, 105943.
[4] Deliali, A., Tainter, F., Ai, C., Christofa, E.: "A framework for mode classification in multimodal environments using radar-based sensors", Journal of Intelligent Transportation Systems, 2023, 27(4), 441–458.
[5] Dash, I., Abkowitz, M., Philip, C.: "Factors impacting bike crash severity in urban areas", Journal of Safety Research, 2022, 83, 128–138.
[6] Bahrololoom, S., Young, W., Logan, D.: "Modelling injury severity of bicyclists in bicycle-car crashes at intersections", Accident Analysis & Prevention, 2020, 144, 105597.

© 2023 Copyright by DYNAmore GmbH, an Ansys Company

[7] Peng, Y., Chen, Y., Yang, J., Otte, D., Willinger, R.: "A study of pedestrian and bicyclist exposure to head injury in passenger car collisions based on accident data and simulations", Safety Science, 2012, 50(9), 1749–1759.
[8] Gao, W., Bai, Z., Zhu, F., Chou, C. C., Jiang, B.: "A study on the cyclist head kinematic responses in electric-bicycle-to-car accidents using decision-tree model", Accident Analysis & Prevention, 2021, 160, 106305.
[9] Huang, Y., Zhou, Q., Koelper, C., Li, Q., Nie, B.: "Are riders of electric two-wheelers safer than bicyclists in collisions with motor vehicles?", Accident Analysis & Prevention, 2020, 134, 105336.
[10] Maki, T.: "The behavior of bicyclists in frontal and rear crash accidents with cars", JSAE Review, 2001, 22(3), 357–363.
[11] Carmai, J., Koetniyom, S., Hossain, W.: "Analysis of rider and child pillion passenger kinematics along with injury mechanisms during motorcycle crash", Traffic Injury Prevention, 2019, 20(sup1), S13–S20.
[12] Terashima, T., Kato, K., Oga, R., Takubo, N., Mizuno, K.: "Experimental study on car collisions with bicycles equipped with child seats", Accident Analysis & Prevention, 2022, 166, 106535.
[13] Zander, O., Hamacher, M.: "REVISION OF PASSIVE PEDESTRIAN TEST AND ASSESSMENT PROCEDURES TO IMPLEMENT HEAD PROTECTION OF CYCLISTS", 25th International Technical Conference on the Enhanced Safety of Vehicles, 2017, 17-0376.
[14] Pal, C., Hirayama, S., Vallabhaneni, P. N., Vimalathithan, K., Manoharan, J.: "Comparison of head kinematics of bicyclist in car-to-bicycle impact", WCX SAE World Congress Experience, 2020, 2020-01-0932
[15] Katsuhara, T., Miyazaki, H., Kitagawa, Y., Yasuki, T.: "Impact Kinematics of Cyclist and Head Injury Mechanism in Car-to-Bicycle Collision", IRCOBI Conference, 2014, 670-684.
[16] Pal, C., Vallabhaneni, P., Kulothungan, V., Manoharan, J., Shigeru, H.: "Af05 bicyclist's head kinematics in car-to-ebike perpendicular and angular impacts", International Journal of Automotive Engineering, 2021, 12(1), 16–23.
[17] Monfort, S. S., Mueller, B. C.: "Bicyclist crashes with cars and SUVs: Injury severity and risk factors", Traffic Injury Prevention, 2023, 24(7), 645–651.
[18] Siegler, S., Allard, P., Kirtley, C., Leardini, A., Rosenbaum, D., Whittle, M., D'Lima, D., Cristofolini, L., Witte, H., Schmid, O., Stokes, I.: "ISB recommendation on definitions of joint coordinate system of various joints for the reporting of human joint motion—part I: ankle, hip, and spine", Journal of Biomechanics, 2002, 543-548.
[19] Wu, G., Van der Helmb, F., Veeger, H., Makhsous, M., Van Roy, P., Anglin, C., Nagels, J., Karduna, A., McQuade, K., Wang, X., Werner, F., Buchholz, B.: "ISB recommendation on definitions of joint coordinate systems of various joints for the reporting of human joint motion—Part II: shoulder, elbow, wrist and hand", Journal of Biomechanics, 2005, 981-992.
[20] Klein, C., González-García, M., Weber, J., Bosma, F., Lancashire, R., Breitfuss, D., Kirschbichler, S., Leitgeb, W.: "A Method for Reproducible Landmark-based Positioning of Multibody and Finite Element Human Models", IRCOBI Conference, 2021, 477-489.
[21] Frostell, A., Hakim, R., Thelin, E., Mattsson, P., Svensson, M.: "A Review of the Segmental Diameter of the Healthy Human Spinal Cord ", Frontiers in Neurology, 2016.
[22] Gilad, I., Nissan, M.: " Sagittal evaluation of elemental geometrical dimensions of human vertebrae", Journal of Anatomy, 1985, 115-120.

© 2023 Copyright by DYNAmore GmbH, an Ansys Company